Tunnelling and Underground Space Technology incorporating Trenchless Technology Research xxx (xxxx) xxx-xxx

Contents lists available at ScienceDirect

Tunnelling and Underground Space Technology

journal homepage: http://ees.elsevier.com

Factors influencing overbreak volumes in drill-and-blast tunnel excavation. A statistical analysis applied to the case study of the Brenner Base Tunnel – BBT

G.M. Foderà [a], A. Voza [a], G. Barovero [a], F. Tinti [b], D. Boldini [c,d,*]

[a] Galleria di Base del Brennero - Brenner Basistunnel BBT-SE, Piazza Stazione 1, 39100 Bolzano, Italy
[b] University of Bologna, Department of Civil, Chemical, Environmental and Materials Engineering, via Terracini 28, 40131 Bologna, Italy
[c] Sapienza University of Rome, Department of Chemical Engineering Materials Environment, via Eudossiana 18, 00184 Rome, Italy
[d] Formerly University of Bologna, Department of Civil, Chemical, Environmental and Materials Engineering

ARTICLE INFO

Keywords
Brenner Base Tunnel
Geological overbreak
Technical overbreak
Rock Mass Rating
Blast hole length
Statistical analysis

ABSTRACT

This paper deals with the analysis of overbreak in tunnels excavated with the drill-and-blast method. The overbreak phenomenon has many negative impacts on tunnelling organisation and economy and its precise assessment plays a fundamental role in the process of construction optimisation. The study proposes an operative methodology to estimate overbreak volumes and to distinguish so-called technical overbreak, mainly related to drill-and-blast design and execution, from geological overbreak, typically influenced by rock-mass characteristics. The approach was developed and implemented during the excavation of the Brenner Base Tunnel (BBT) and was based on the interpretation of tunnel laser scanning surveys and high-resolution images of the excavated surfaces. The analysis of more than 1,800 m of excavation from three different tunnels of the BBT system allowed to identify the main factors influencing the technical and the geological overbreak. An empirical model for overbreak prediction, based on the Rock Mass Rating index and the length of blast holes, is subsequently presented and validated in the last part of the paper.

1. Introduction

Drill-and-blast excavation is still widely used in mining, quarrying and hard rock tunnelling for its relatively low costs and efficiency and feasibility of implementation (Verma et al., 2018). However, this method has the inherent disadvantage of damaging the rock-mass around the excavated section, possibly resulting in the development of blast-induced undesired cavities. This phenomenon is called "overbreak". Overbreak impacts underground constructions mainly with the following issues: potentially unstable rock-mass, increased cost of support systems, slow advancement rate and higher post-construction maintenance cost, mainly related to possible water seepage through unfilled voids at the lining extrados (Verma et al., 2018). Therefore, the prediction and the minimisation of overbreak during excavation is a challenging task in any tunnelling and mining project. A number of researchers have analysed the factors influencing the undesired excavation induced by blasting (Ibarra et al., 1996; Singh and Xavier, 2005; Mandal and Singh, 2009; Van Eldert, 2017). In this respect, overbreak can be roughly divided into two main categories: so-called "geological overbreak", caused by geomechanical features of the rock-mass, and "technical overbreak", related to drill-and-blast design and execution. While geological overbreak may be predicted by investigating the rock-mass characteristics, though hardly avoided, technical overbreak can also be controlled by adopting appropriate blasting techniques (Hoek and Brown, 1980).

Referring to the impact of different explosives on technical overbreak, Widodo et al. (2019) compared conventional Ammonium Nitrate Fuel Oil (ANFO) and emulsion explosives. The two explosives were adopted in various tunnels of the underground sector of the Grasberg Gold Mine in Indonesia, excavated in a diorite formation. ANFO and emulsion explosives generated different quantities of overbreak and underbreak. More specifically, the emulsion produced some underbreak and little overbreak, while the ANFO application was characterised by a higher overbreak and limited underbreak volumes.

The precise prediction of overbreak extent and the quantification of impacts, both technical and economical, is still an object of discussion. Mahtab et al. (1997) proposed an analytical approach to assess, for a given level of confidence, admissible thresholds of the geological overbreak, starting from the uncertainty related to the main rock-mass characteristics. Their approach is based on the two-dimensional limit equilibrium analysis of rock wedges at the perimeter of the excavation, with normal and shear stresses along the joints calculated on the ba-

* Corresponding author at: Sapienza University of Rome, Department of Chemical Engineering Materials Environment, via Eudossiana 18, 00184 Rome, Italy.
E-mail address: daniela.boldini@uniroma1.it (D. Boldini)

https://doi.org/10.1016/j.tust.2020.103475
Received 26 July 2019; Received in revised form 29 May 2020; Accepted 2 June 2020
Available online xxx
0886-7798/

sis of the stress field around a circular hole in an anisotropic elastic medium. Other authors attempted a correlation between the rock-mass quality, quantified in terms of rock-mass rating (*RMR*) and rock quality designation (*RQD*) indexes, and the overbreak volume assessed by topographic surveys (Innaurato et al., 1998; Schmitz et al., 2006). Dey and Murthy (2012) developed a composite blast-induced rock damage predictive model starting from rock-mass parameters, blast design parameters and explosive charge parameters, successively validated with laboratory and field investigations at five tunnels. In this model, P-wave velocity of rock-mass and, quite surprisingly, Poisson's ratio were considered as the relevant rock-mass quality parameters. Specific charge at the tunnel boundary, excavation round length and charge confinement in the borehole were selected as the charge and blast descriptors. Gong et al. (2008) applied a statistical approach, based on the Bayes discriminant analysis, for the prediction of overbreak and its discriminant factors. Eight specific parameters, four referring to the orientation of two dominant joint sets (dip direction and dip angles of joints 1 and 2), two referring to the orientation of the excavation surface (dip direction and dip angles) and the last two referring to the extension and spacing of discontinuities, were adopted as geometric parameters capable of influencing the over-excavation. Cross-validation was used to estimate the reliability of the Bayes discriminant criterion. Jang and Topal (2013) compared the quality of three regression methods, by the determination coefficient R^2 between the measured and predicted overbreak values: linear multiple regression analysis, with five variables (unconfined compressive strength of rock, *RQD*, *RMR*, spacing of joints and conditions of joints), nonlinear multiple regression analysis with two variables (joint spacing and orientation) and artificial neural network with one variable (*RMR*). Results indicated the artificial neural network as the best method for the specific case study. Mohammadi et al. (2018) applied a linear multiple regression on nine parameters, two geomechanical and seven technical, to evaluate their impact on the overbreak. Reference was made to four tunnels of the Bakhtiari dam, located in Iran, excavated with drill-and-blast method in a limestone rock-mass, where smooth blasting was applied. The model was validated on 24 overbreak data sets and the resulting parameters were provided in terms of statistics (min, max, average and standard deviation). In addition, presence of autocorrelation and multicollinearity among parameters was checked using the Durbin-Watson statistical index. Results showed that the Rock Tunnelling Quality Index, the perimeter charge, the cross-sectional area of the tunnel face and the burden to spacing ratio of the contour blast holes are the main factors affecting the overbreak. No distinction between technical and geological overbreak was accounted for. Finally, Kim and Moon (2013) developed specific guidelines for practitioners to decrease the risk of overbreak in drill-and-blast projects, specific for reducing the occurrence of technical errors and maintaining the impact of technical overbreak under control. The guidelines provide indications on the geometry of the blast hole drilling and the charge of explosives in relation to the rock mass quality. They were applied in the context of field tests carried out in four tunnels in South Korea, showing their effectiveness, with an overbreak reduction from 10% to 77% with respect to standard practices. The additional time needed for workers to implement the new procedures was calculated to be about 10 min per tunnel excavation round; therefore, the Authors judged it negligible in the context of drill-and-blast tunnelling projects.

The present paper analyses the case study of the Brenner Base Tunnel (BBT), currently under construction through the Alps between Italy and Austria (www.bbt-se.com; see also Boldini et al., 2018; Voza et al., 2020 for some other technical details). The study proposes an operative methodology to distinguish the technical from the geological overbreak and to perform reliable previsions on the basis of a high amount of data of different origin (surveys and laser scanning). The influence of the most important parameters was assessed by a multiple regression analysis to find empirical relations of overbreak occurrence with both technical and geomechanical parameters. The accuracy of overbreak volume prediction was validated by measurements collected at different tunnels of the BBT system.

2. Materials and methods

2.1. The overbreak phenomenon

Fig. 1 shows a view of the theoretical tunnel section and two possible situations often occurring in practice during drill-and-blast excava-

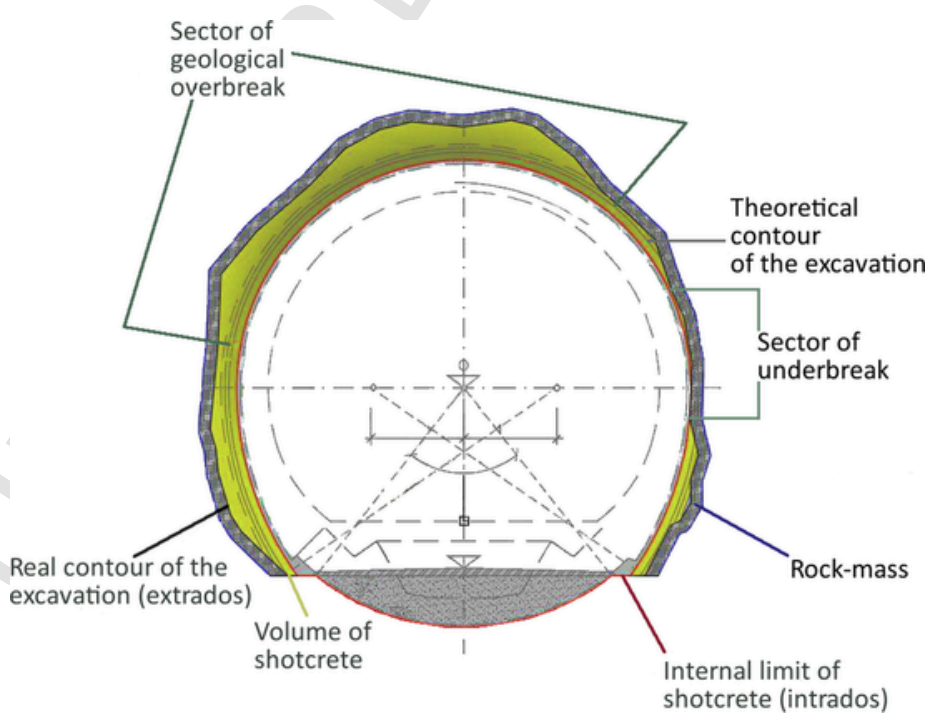

Fig. 1. Scheme of the theoretical and real tunnel profile, with evidence of overbreak and underbreak volumes.

tion: the so-called "overbreak", which corresponds to the rock volume excavated in excess with respect to the design profile, and the "underbreak", which, on the contrary, indicates the rock volume internal to the desired tunnel clearance. Typically, the first condition (i.e. the overbreak) occurs more frequently than the second one (i.e. the underbreak) and is characterised by larger volumes.

Geometry and amount of overbreak depend on many factors, which can be grouped into two families: those affecting "technical overbreak", depending essentially on the excavation technique, and those controlling "geological overbreak", which are essentially related to the rock-mass characteristics.

Technical overbreak, typically affecting limited and cortical rock-mass volumes, is dependent on the inaccuracy in drilling and loading of contour blast holes, which control the damage induced in the surrounding rock-mass during blasting.

In contrast, geological overbreak is related to the local rock-mass conditions, possibly promoting rock wedge failure mechanisms. The principal rock-mass characteristics influencing geological overbreak are:

1. Number, orientation and properties of the discontinuities at the tunnel face;
2. In situ state of stress, which is released abruptly during the excavation and can contribute to the detachment of rock blocks.

The negative effects of the overbreak phenomenon are essentially proportional to the overbreak volume. The dominant issue concerns the economy: the higher the overbreak, the larger the volume of spoil material to be disposed of and the larger the size of the cavities to be filled with shotcrete. For various technical reasons, mainly due to the desire to avoid a second re-profiling excavation, underbreak is rarer than overbreak and tends to be prevented. Therefore, excess volume of excavation (overbreak) may be frequent and the additional costs should be accounted for a correct estimation of the total excavation. The economic loss varies according to the type, dimension and geometry of the tunnel.

Overbreak additional costs are frequent cause of disputes between the client and the construction company. Therefore, some regulations have been attempted in tunnel projects to assess the economic impact of overbreak, trying to separate geological overbreak (typically borne by the client) from technical overbreak (the responsibility for which is often ascribed to the construction company). Typically, construction tolerances of the theoretical excavation profile are considered in the design phase of both first and second phase linings. Each tolerance represents an admissible deviation between theoretical and effective excavated volume and should be taken into account in the analysis of the overbreak.

Tunnel laser scanning (TLS) is being increasingly used as a survey and monitoring technique in tunnel construction and management, since it provides useful information, such as the detailed inspection of the completed tunnel geometry, the conformity of the ripples to the design tolerance and the precise assessment of shotcrete and cast in place concrete thicknesses (Sorce et al., 2019). Currently, TLS is the common method used to measure the total volume of excavation, and thus of overbreak. TLS produces a 3D point cloud representing the surface of the tunnel walls, thus allowing the definition of the actual geometry for each tunnel excavation round. Additionally, standard survey data are usually integrated with the 3D point cloud to complete the information acquired from TLS. The high number of measured data and the reconstruction of a 3D model are useful for the identification of the overbreak volumes with a high level of precision. The quality of the measurements is affected by the scanner's field of view, which can be limited by the presence of facilities (air ducts, electricity cables, …), vehicles (dumpers, jumbos, …) and reflective surfaces (puddles and water incomes).

2.2. Application to the BBT case study

The Brenner Base Tunnel (BBT), part of the European Corridor TEN SCAN-MED, is an Alpine railway link, currently under construction, that will connect the town of Fortezza (Italy) to the city of Innsbruck (Austria). The overall infrastructure length is about 55 km and the entire project will require the construction of about 230 km of tunnels, under variable overburdens, ranging from few metres to about 1700 m. The tunnels start at an elevation of 743 m a.s.l. at Fortezza, rising to a peak at 794 m a.s.l. near the Brenner pass, and finally reaching the city of Innsbruck at 609 m a.s.l. (www.bbt-se.com). Scheduled to become operational in 2026, the project includes the construction of:

- 2 (in progress) main single-direction railway tunnels, characterised by a diameter of about 9 m, referred to as the East and West tunnels;
- 1 (in progress) exploratory tunnel excavated in advance for geological and geomechanical investigation, with a diameter of about 6 m;
- 4 (almost completed) access tunnels (Ampass, Ahrental, Wolf and Mules/Trens) used for logistics during the tunnel construction and as emergency escape routes when the tunnel system will be operational;
- 3 (planned) emergency stations (Innsbruck, St. Jodok and Campo di Trens).

The BBT tunnels run through many different geological units and several faults. The zones considered in the present research are south of the Periadratic Seam, part of the Mules 2/3 area. In this area, hard rock conditions (mainly Brixner granite) are predominant and the drill-and-blast excavation method was more frequently adopted. Fig. 2 contains the geological planimetry of the Brenner Pass, showing the route of the new railway tunnel (in yellow) and the area under investigation (with a green box).

In the following, we refer to three tunnels: the Mules/Trens access tunnel to the emergency station of Campo di Trens (known as "Galleria di Accesso" - GA), the exploratory tunnel (known as "Cunicolo Esplorativo" - CE) and one of the main southwest tunnels (known as "Galleria di Linea Sud Ovest" - GLOS). For the scope of the present study, only the tunnel portions excavated by drill-and-blast were considered (clearly indicated in Fig. 3).

The geomechanical conditions of the investigated tunnel segments can be summarised as follow:

- GA: the first part is excavated through Brixner granite with *RMR* greater than 70; the second portion crosses the highly disturbed Val Pusteria fault zone with *RMR* ≈ 45; the third part runs through Mules tonalite with *RMR* ≈ 55.
- CE: the first part is adjacent to the Mules fault and is mainly formed by highly disturbed micaschist with *RMR* ≈ 45; the second portion mainly consists in less disturbed paragneiss and quartz micaschist, with *RMR* ≈ 55.
- GLOS: the rock-mass is entirely constituted by massive Brixner granite with an *RMR* index greater than 70.

The related geological sections are represented in Fig. 4(A)–(C), respectively.

All three tunnels (GA, CE and GLOS) were excavated adopting the same drill-and-blast scheme and ignition sequence (Fig. 5), whose main characteristics are:

- blast hole diameter 0.051 m;
- spacing of contour blast holes of zone 1 0.81 m;

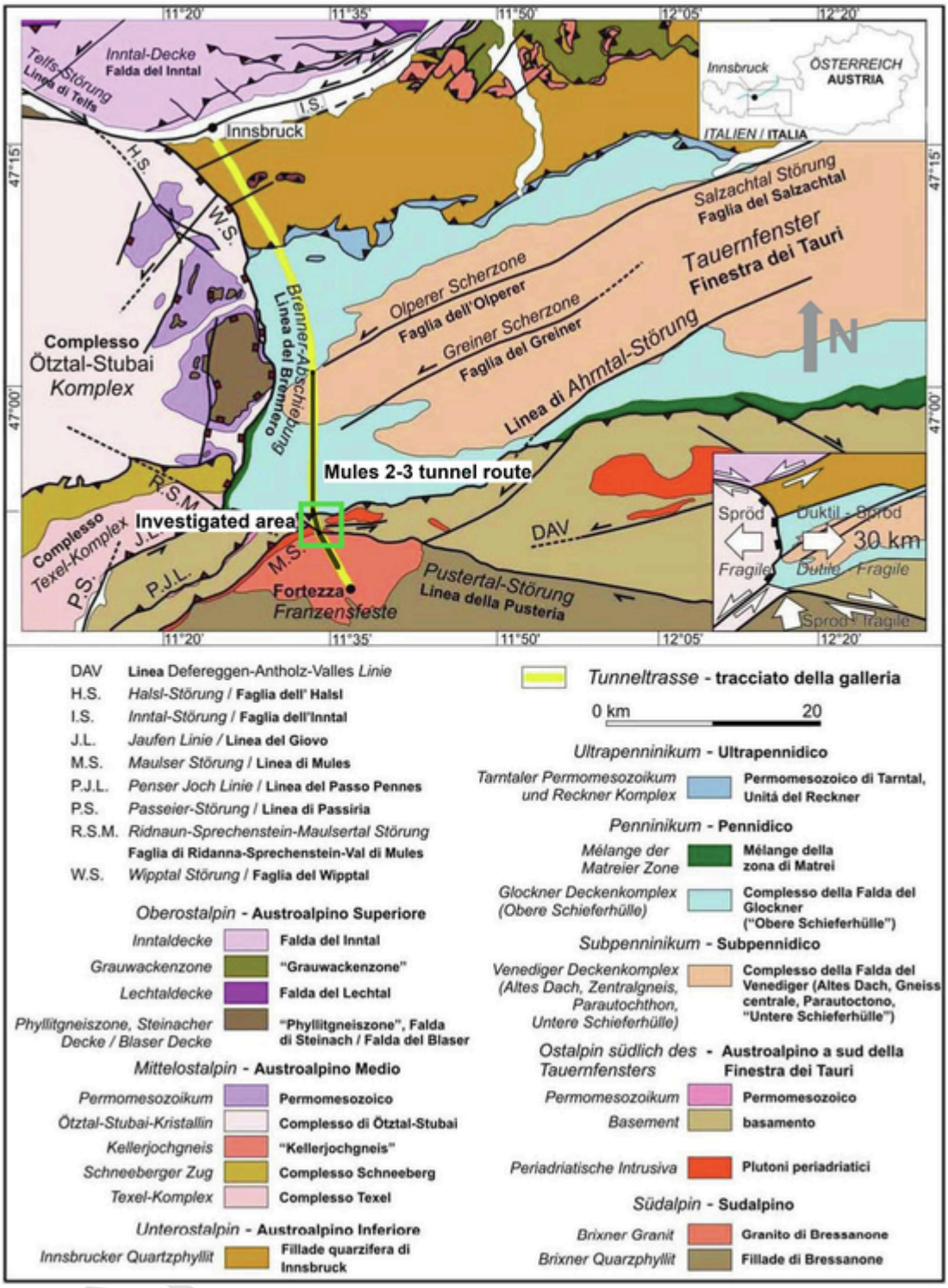

Fig. 2. Geological planimetry of the Brenner Pass (the tunnel route and the investigated area are also visible).

- spacing of contour blast holes of zone 2 varying between 0.70 and 0.90 m;
- total number of blast holes 115;
- density of blast holes 1.7 per m^2;
- length of the blast holes variable between 1.5 and 5.0 m;
- explosive types emulsion cartridge riohit Ø40, dynamite cartridge riodin Ø40, detonating cord 80 g/m;
- decoupling for contour blast holes high in zone 1 and low in zone 2, with respect to diameter of the blast hole.

The ignition sequence is characterized by micro-delays and is divided into two areas: the internal one (red bold type numbers in Fig. 5), with variable micro-delays from 25 ms to 300 ms, and the external one, with constant micro-delays of 100 ms.

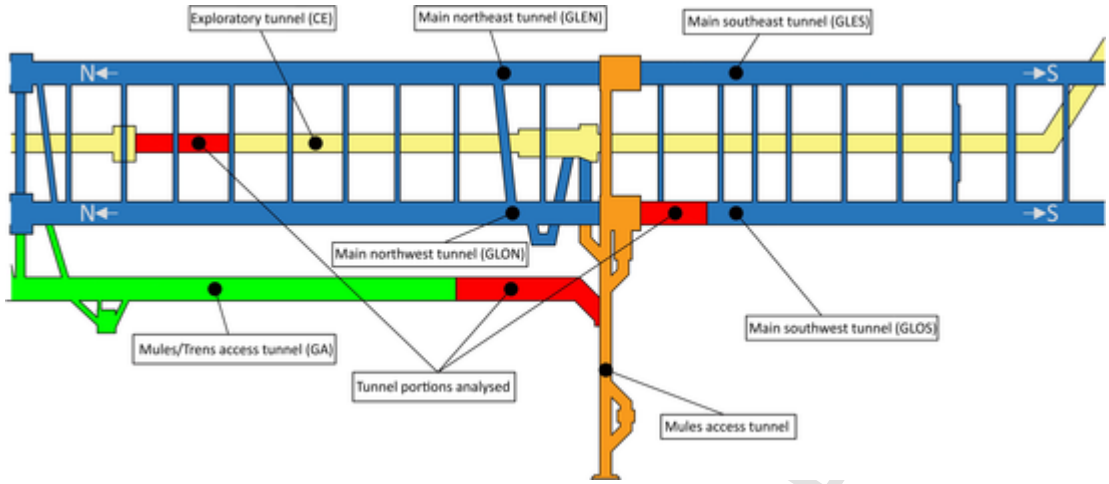

Fig. 3. Scheme of the Mules 2–3 area and location of the three analysed tunnel segments.

As an example, for a length of the blast holes equal to 3 m, the charge details reported in Table 1 were implemented. In addition, the following details were carried out:

- Blast holes n°20 and 25, located at the top of zone 1, are charged by a dynamite cartridge at bottom hole and 3 detonating cords. The total charge in each blast hole is 0.95 kg. These blast holes are used to perform the smooth blasting in zone 1 to profile the excavation contour limiting the damage of surrounding rock mass. The specific design of these perimeter blast holes, together with the charge decoupling, allows guided detachment of the rock along a fracture propagating among the holes, thus preserving the adjacent medium.
- Blast holes n°30, 35, 40 and 45, located at the bottom of zone 2, are charged by 3 emulsion and 1 dynamite cartridges, for a total charge in each blast hole of 3.21 kg.
- All the other blast holes are charged by 3 emulsion cartridges for a total charge in each blast hole of 2.5 kg.

The total charge for the tunnel section is 262.79 kg. Proportional values were adopted for the other lengths of the blast holes analysed in this work.

Fig. 6 summarises the scheme adopted by BBT-SE to define the theoretical excavation contour ("line 2" in the picture). Over "line 2", overbreak occurs. However, two tolerances are admissible: d_1 is the extra excavation tolerance to account for the deformations of the rock-mass (convergences), while d_2 is the so-called technical tolerance due to issues related to the excavation method. The thickness of d_1 for the tunnels considered here is 5 cm, while the values of d_2 are reported in a specific table prepared by BBT, divided according to the excavation technique and the tunnel section type (Table 2).

The three analysed tunnel portions differ significantly one from another in terms of geological, geomechanical and geometrical characteristics. Most data refer to the portion of the GA tunnel, being the longest among the investigated ones.

Comparisons among 3D point cloud from TLS, photographs and geological surveys carried out at the tunnel face were performed in order to reliably distinguish geological from technical overbreak volumes. Controlled-blasting techniques, when effective, leave intact almost half the blast hole surface, referred to as "half-casts" or "half-barrels". Half casts are the traces of blast holes on the excavated surfaces, and they are often associated with radial fractures, provoking a blast-induced damaged zone from 0.3 to 0.5 m thick (Saiang, 2008) (Fig. 7). Therefore, the so-called Half Cast Factor (*HCF*) is a popular parameter for the assessment of induced damage. It is computed as the total length of visible half-casts divided by the total length of drilled contour blast holes, and is typically expressed as a percentage (McKown, 1986):

$$HCF = \frac{\sum_{i=1}^{n} L_i}{\sum_{r=1}^{n} L_r} \text{x } 100 \ (\%) \tag{1}$$

where L_i is the generic post-blast visible half cast and L_r is the pre-blast drilling length.

This methodology, developed by the Swedish Rock Engineering Research (Andersson, 1992; Olsson and Berqgvist, 1997, quoted in Saiang, 2008), was applied to differentiate between blast-induced overbreak and that associated with other sources, either natural or stress-induced. When the overbreak occurred in a zone of visible half-casts ($HCF > 0$), then technical overbreak was indicated as the main component; on the contrary, when the overbreak was observed in the absence of visible half-casts ($HCF = 0$), it was assumed to be influenced by geological aspects (Fig. 8). The application of this procedure was practically feasible due to the implementation of the smooth blasting technique in the BBT tunnels, causing the rock-mass to break only at the intrados, while preserving visible half-casts at the extrados.

The proposed approach seems coherent with the physical phenomena occurring during the drill-and-blast excavation. The procedure is not automatic and implies the integration of measurements of different type and extension. Identification of half-casts requires visual survey along the tunnel surfaces, thus leading to potential errors. Moreover, because of limitations in the field of view of TLS, due to the presence of vehicles and reflecting surfaces during the excavation phase, measurements were not continuously available. For all these reasons, significant pre-processing work on the data was necessary.

More than 2,000 excavation profiles were collected via TLS and analysed. More than 430 geological surveys of the tunnel face were also available and integrated with the profiles obtained using TLS for the half-cast identification and subsequent evaluation of overbreak volumes. Table 3 summarises the number of investigated tunnel sections, while Table 4 shows the effective measurements of overbreak used for the present work, together with basic information on the three tunnels.

The study focused initially on the GA tunnel, being the longest one and with the largest number of overbreak measurements. The total sections analysed were 276, with different excavation round length L_s (m), comprised between 1.5 and 5.0 m and with the majority of values equal or above 3.0 m (63.4%). Table 5 provides the details of the L_s frequency for the analysed GA tunnel sections.

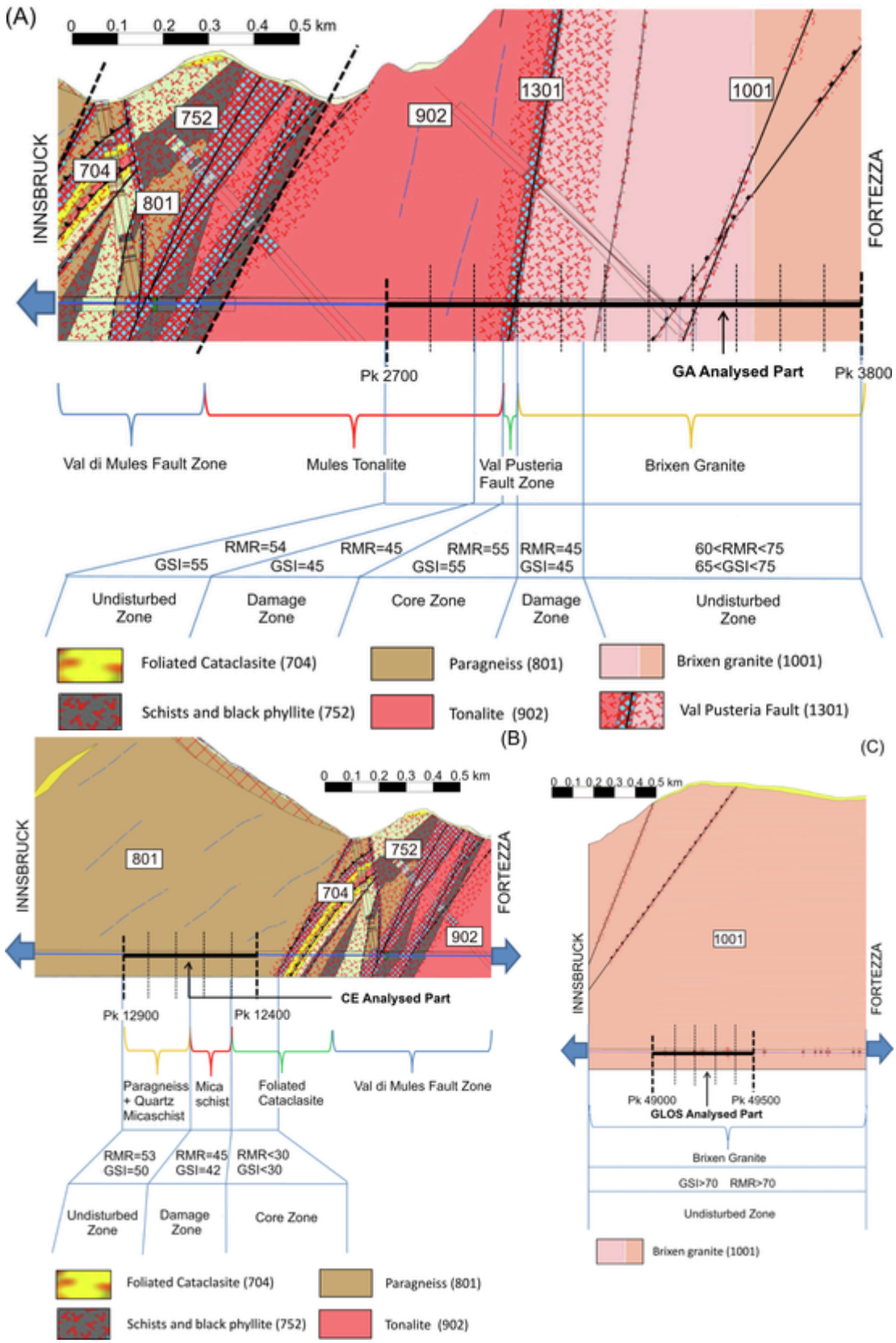

Fig. 4. Geological sections with the investigated portions of the GA (A), CE (B) and GLOS (C) tunnels.

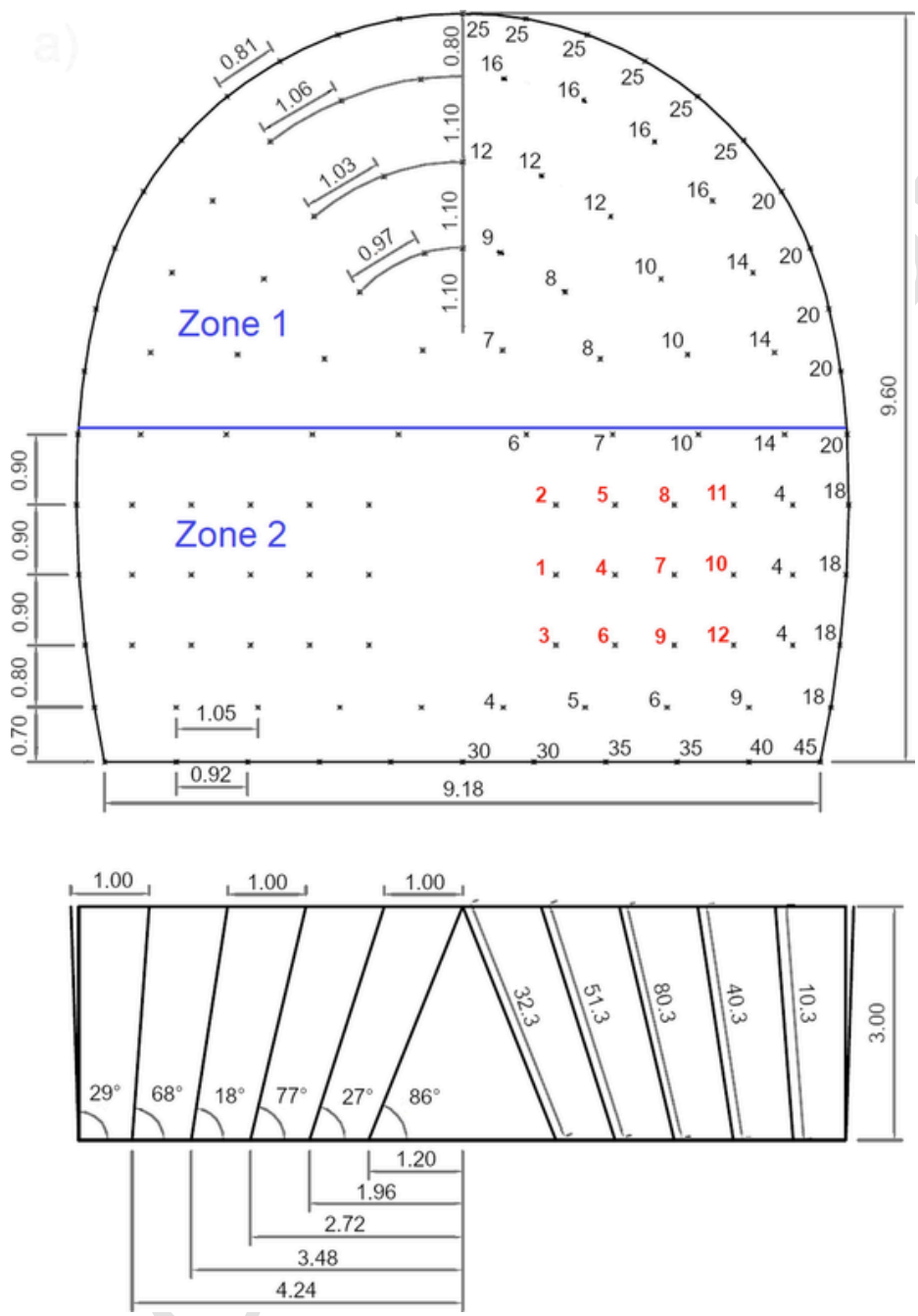

Fig. 5. Drill-and-blast scheme and ignition sequence valid for all the analysed section types (a perfectly symmetric arrangement is adopted for the left and right portions of the section).

3. Statistical analysis

For each excavation cycle, the volume of overbreak V_{ob} was calculated as the product of the measured area of overbreak A_{ob}, determined by the TLS, and the extent of excavation round length.

$$V_{ob} = A_{ob} \cdot L_s \tag{2}$$

As discussed before, the total volume of overbreak is composed by two parts: technical overbreak $V_{ob,tec}$ and geological overbreak $V_{ob,geo}$. Therefore, V_{ob} can be calculated also as follows:

$$V_{ob} = V_{ob,tec} + V_{ob,geo} \tag{3}$$

In order to compare the overbreak data for the three tunnels, characterised by different diameters, the specific overbreak OB was considered instead. It is defined as the ratio between the volume of overbreak V_{ob} and the theoretical volume of excavation V_{exc}:

$$OB = \frac{V_{ob}}{V_{exc}} \tag{4}$$

TLS measurements were interpreted to precisely measure the tunnel surface for each section. The areas delimited by the presence of half-casts were extracted, thus obtaining the average volume of the technical overbreak for each tunnel section. Subsequently, the geological overbreak was calculated by measuring the exceeding volumes. On the parts of the tunnel contour affected by geological overbreak, half-casts are not visible so the distinction between technical and geological overbreak is not strictly possible. Consequently, the identified geological overbreak comprised also part of the technical one and the sum of mea-

Table 1
Details of the blast hole charge.

Delay number	Blast hole charge					N° of blast holes for delay	Charge for delay (kg)
	Cart. Riohit XE Ø 40	Cart. Riodin XE Ø 40	Cart. Riohit LS Ø 40	Detonating cord 80 g/m	Charge weight (kg)		
1	3	0	0	0.0	2.50	2	5.00
2	3	0	0	0.0	2.50	2	5.00
3	3	0	0	0.0	2.50	2	5.00
4	3	0	0	0.0	2.50	2	5.00
5	3	0	0	0.0	2.50	2	5.00
6	3	0	0	0.0	2.50	2	5.00
7	3	0	0	0.0	2.50	2	5.00
8	3	0	0	0.0	2.50	2	5.00
9	3	0	0	0.0	2.50	2	5.00
10	3	0	0	0.0	2.50	2	5.00
11	3	0	0	0.0	2.50	2	5.00
12	3	0	0	0.0	2.50	4	10.00
4	3	0	0	0.0	2.50	5	12.50
5	3	0	0	0.0	2.50	5	12.50
6	3	0	0	0.0	2.50	4	10.00
7	3	0	0	0.0	2.50	4	10.00
8	3	0	0	0.0	2.50	4	10.00
9	3	0	0	0.0	2.50	4	10.00
10	3	0	0	0.0	2.50	6	15.00
12	3	0	0	0.0	2.50	5	12.50
14	3	0	0	0.0	2.50	6	15.00
16	3	0	0	0.0	2.50	8	20.00
18	3	0	0	0.0	2.50	8	20.00
20	0	1	0	0.0	0.95	10	9.50
25	0	1	0	3.0	0.95	11	10.50
30	3	1	0	3.0	3.21	3	9.60
35	3	1	0	0.0	3.21	4	12.90
40	3	1	0	0.0	3.21	2	6.40
45	3	1	0	0.0	3.21	2	6.40
						115 Number of blast holes	**262.79** Total charge (kg)

sured $V_{ob,tec}$ and $V_{ob,geo}$ is affected by a systematic error, with the calculated total overbreak volumes larger than the actual ones. The same error also affects the specific geological overbreak OB_{geo}.

3.1. Initial correlations among variables

The first step of the work consisted in investigating the possible correlations among OB_{tec} and OB_{geo} values and the main factors influencing the technical and geological overbreak. Given the different excavation round lengths, varying from 1.5 to 5.0 m (see Table 5), a method was needed to regularise the *OB* data, so as to analyse them consistently. The new regularised *OB* values were obtained by choosing a constant support equal to the maximum length of 5.0 m and then by calculating the weighted average of measurements over their dimension. The list of considered parameters is presented in Table 6 together with the calculated correlation coefficients.

Inspection of Table 6 reveals that, as expected, technical overbreak is highly directly correlated with the length of the blast holes L_{blast} (ρ = 0.51): since the blast holes are inclined, the offset from the horizontal direction increments with the length, thus increasing the probability of overexcavation. Geological overbreak, on the contrary, was found to be highly directly correlated with the number of families of discontinuities (ρ = 0.42) and inversely correlated with global rock-mass quality, represented by the *RMR* index (ρ = -0.62).

L_{blast} and *RMR* index were therefore identified as those parameters most affecting the overbreak phenomenon and as such selected for further analyses. Several regression models were attempted to find the best fit, quantified by the determination coefficient R^2, between the specific technical overbreak and L_{blast}, on one side, and the specific geological overbreak and the *RMR* index, on the other side. Results are summarised in Table 7 and show that in the former case the best fit is given by a power law (Fig. 9) while in the latter case by a logarithmic law (Fig. 10). It is worth noting that the simple linear law is also characterised by comparable determination coefficients.

Other parameters related to rock-mass discontinuities (i.e. number, orientation, spacing and degree of alteration) did not show a significant correlation with the specific geological overbreak (correlation values from 0.00 to 0.20). Other factors, such as the quantity of explosive, the spacing and diameter of contour blast holes and the type of explosive, are supposed to influence the quantity of technical overbreak as well. Nonetheless, given their modest variations in the present case study, it was not possible to find a reliable correlation with the technical overbreak values. The complete set of relations between different technical parameters and geological properties and measurements of technical and geological overbreaks is available in the Appendix.

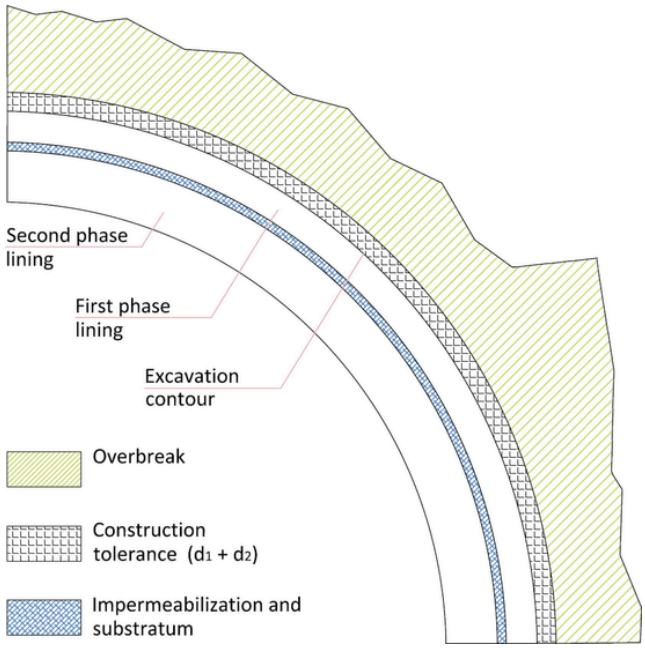

Fig. 6. Schematic representation of design contours and tolerances identified by BBT.

Table 2
Values of d_2 tolerance for the analysed tunnels.

Excavation type	Tunnel name	d_2 tolerance direction	d_2 tolerance value (cm)
Drill and blast	GA	horizontal	±4
		vertical	±2
	CE	horizontal	±35
		vertical	±10
	GLOS	horizontal	±5
		vertical	±2

A similar study was performed on the thickness of the overbreak. For each section, the length of the blast holes as well as the *RMR* index were correlated respectively with the measured average thickness $L_{ob,ave}$, and maximum thickness $L_{ob,\max}$ of the overbreak. More specifically, $L_{ob,ave}$ corresponds to the thickness of the annulus of the technical overbreak, while the difference between $L_{ob,\max}$ and $L_{ob,ave}$ approximately corresponds to the thickness of the annulus of the geological overbreak (Fig. 11).

The statistical correlations (Table 8) and coefficients of the regression (Table 9) are similar to those obtained for the overbreak volume, indicating a limited variability of *OB* along the longitudinal direction for the same excavation round and thus suggesting the possibility of a preliminary overbreak assessment by the only analysis of the thicknesses.

Finally, no evidence of direct correlation between overbreak and tunnel depth was found for any of the analysed tunnels.

3.2. A new overbreak model

The statistical correlations between the specific technical and geological overbreaks and their major factors of influence were found to respectively obey a power and a logarithmic law. As such, an integrated model, given by the linear combination of the previous two, was set up for the calculation of the specific total overbreak:

$$OB = A \cdot \left(L_{blast}\right)^{B} + C \cdot \ln(RMR) + D \tag{5}$$

where *A*, *B*, *C*, *D* are the parameters of the model, to be determined. In the model, L_{blast} should be expressed in m.

Equation (5) refers to the total overbreak normalised to the tunnel theoretical excavated volume to provide a more general expression possibly independent on the specific dimension of the tunnel section. The four parameters were calculated taking into account only the data collected in the Mules/Trens access tunnel (GA), thus disregarding the data available for the CE and GLOS tunnels. This decision was made to subsequently validate the model on data not employed for its initial calibration.

In particular, a nonlinear multiple regression analysis was performed. Initial values of the four regression parameters were set equal to the corresponding ones of the single power and logarithmic regressions of Figs. 9 and 10 (Table 10).

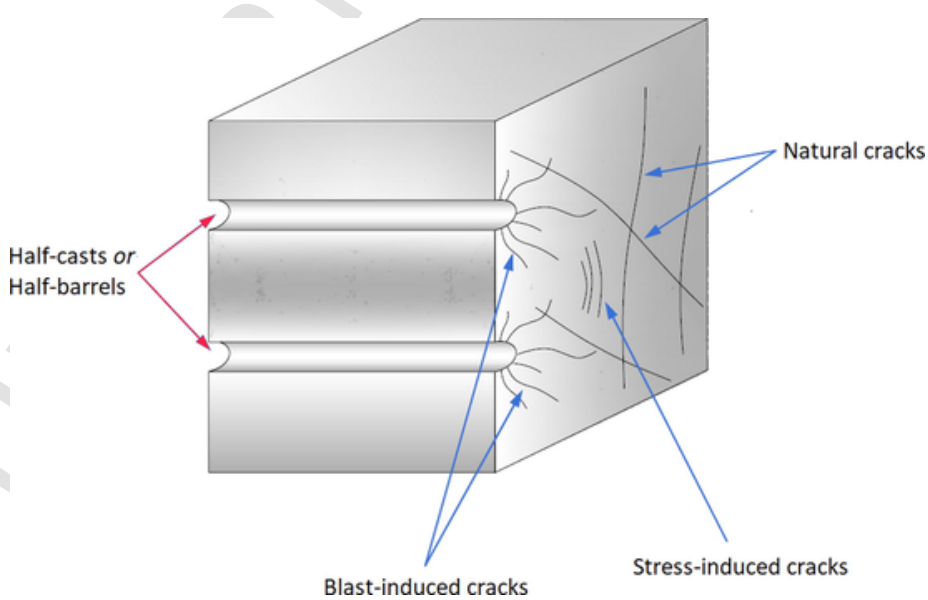

Fig. 7. Scheme of possible cracks visible after blasting (modified from Saiang, 2008).

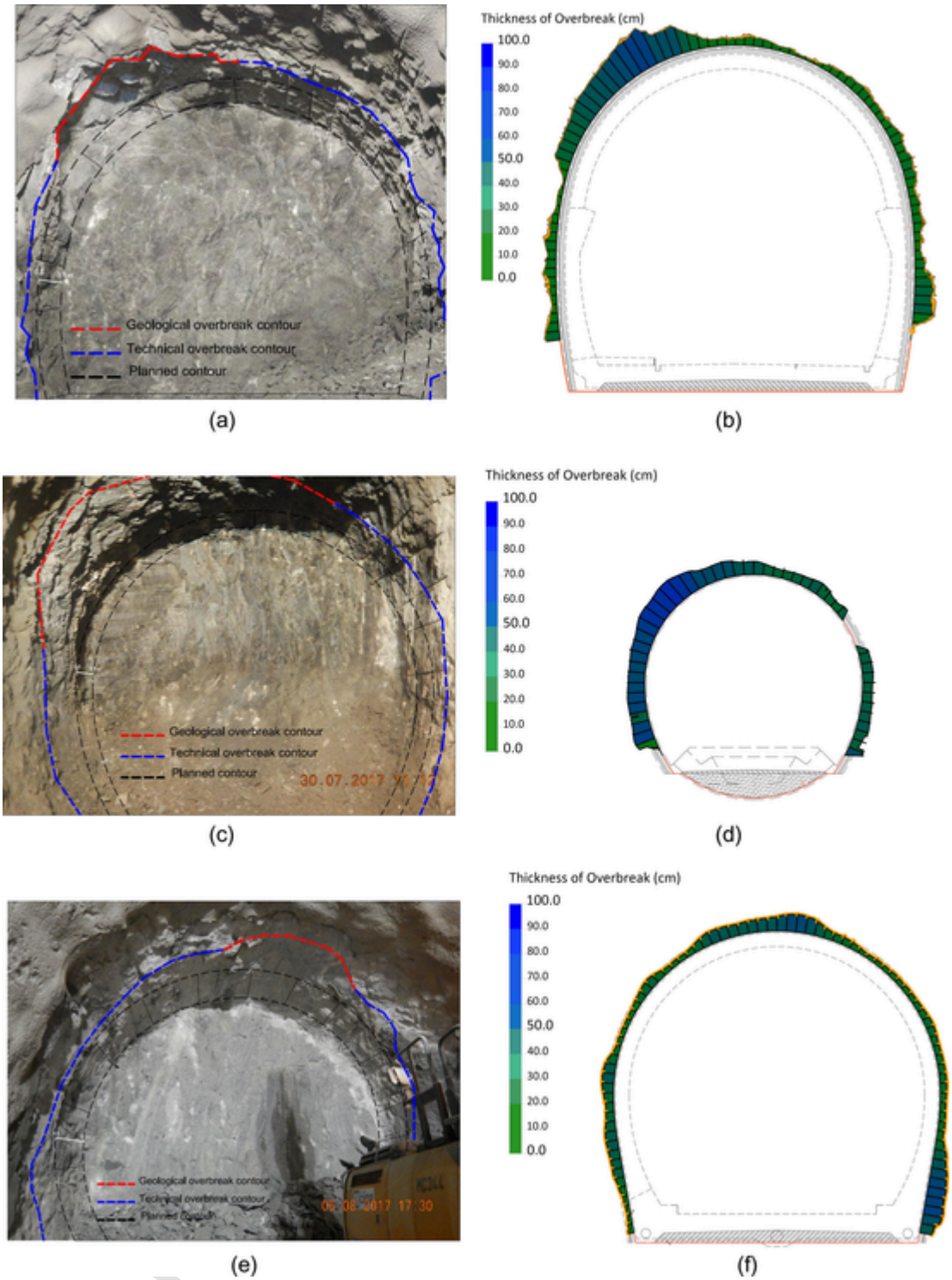

Fig. 8. Comparison between photos and TLS processed images at different tunnel sections, with evidence of planned contour, technical and geological overbreak.

The technique uses the Levenberg–Marquardt algorithm (Levenberg, 1944; Marquardt, 1963) based on differential equations, requiring the calculation of the partial derivatives of Equation (5)

Table 3
Number of investigated tunnel sections subdivided by type and tunnel.

	Tunnel name			
Technique	GA	CE	GLOS	TOTAL
TLS	1,068	616	403	**2,087**
Geological surveys	221	152	61	**434**

Table 4
Number of overbreak measurements used for the present work.

Tunnel name	Length of analysed segment (m)	Theoretical excavation volume per metre of excavation (m^3)	Number of overbreak measurements
GA	1,068	85	116
CE	355	40	10
GLOS	383	65	40

Table 5
Frequency distribution of tunnel sections analysed for the GA tunnel, with respect to the excavation round length.

Excavation round length L_s (m)	Number of analysed tunnel sections	Relative frequency for the analysed tunnel sections
1.5	23	8.3%
2.0	36	13.0%
2.5	42	15.2%
3.0	103	37.3%
3.5	55	19.9%
4.0	12	4.4%
4.5	3	1.1%
5.0	2	0.7%
TOTAL	276	100.0%

Table 6
List of analysed parameters and corresponding correlation coefficients determined for the specific technical and geological overbreak.

Correlation coefficient ρ (data support 5 m)	Specific technical overbreak OB_{tec}	Specific geological overbreak OB_{geo}
Length of the blast holes L_{blast}	+0.51	+0.22
Rock coverage	−0.03	−0.26
Number of families of discontinuities	−0.01	+0.42
Rock quality designation (*RQD*)	−0.17	−0.01
Spacing of discontinuities	−0.16	−0.03
Persistence of discontinuities	+0.14	+0.03
Orientation of discontinuities	−0.17	+0.18
Class of discontinuities	+0.27	−0.17
Rock-mass rating (*RMR*)	+0.18	−0.62
Geological strength index (*GSI*)	+0.01	−0.44

Table 7
Comparison of different models used for the regression statistical analysis of the technical and geological overbreak.

Determination coefficient R^2 (data support 5 m)	Regression of OB_{tec} on L_{blast}	Regression of OB_{geo} on *RMR*
Linear model	0.2629	0.3638
Logarithmic model	0.2654	0.3855
Power model	0.2758	–
Exponential model	0.2719	–

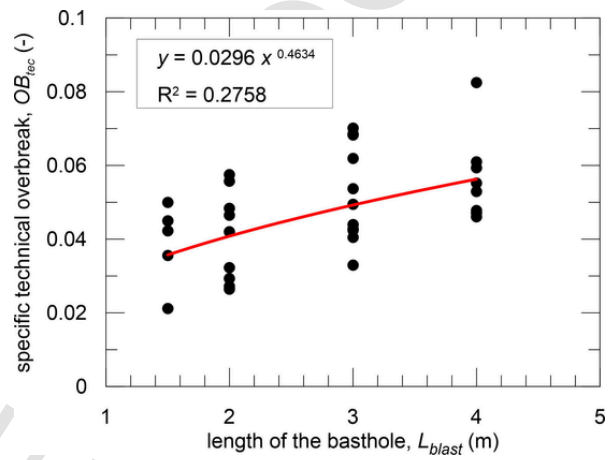

Fig. 9. Relation between length of the blast holes and specific technical overbreak.

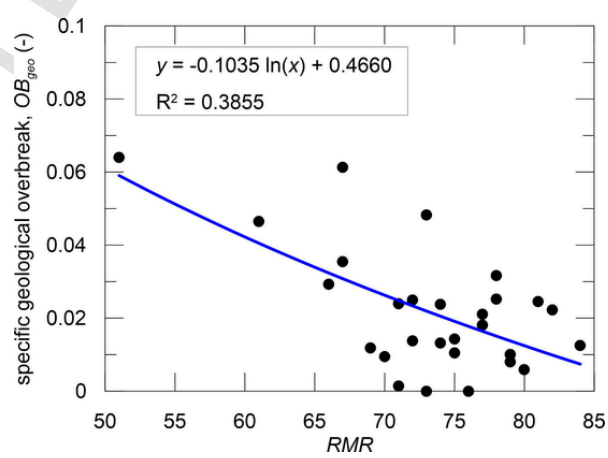

Fig. 10. Relation between the *RMR* index and specific geological overbreak.

with respect to the unknown parameters:

$$\begin{cases} \frac{\partial OB}{\partial A} = \left(L_{blast}\right)^B \\ \frac{\partial OB}{\partial B} = A \cdot \left(L_{blast}\right)^B \cdot \ln\left(L_{blast}\right) \\ \frac{\partial OB}{\partial C} = \ln\left(RMR\right) \\ \frac{\partial OB}{\partial D} = 1 \end{cases} \tag{6}$$

The robustness of results was obtained by imposing a threshold of 0.02 on the allowed standard deviation for each parameter, and then repeating the analysis by selecting only those parameters with a standard deviation above the limit. After the first iteration, the standard deviations of the parameters A and C were found to be below the threshold while those of parameters B and D were well above. A second step was therefore necessary: the A and C parameters were fixed, while the calculation was repeated over the B and D parameters. At the end of the regression procedure, the values for B remained above the thresh-

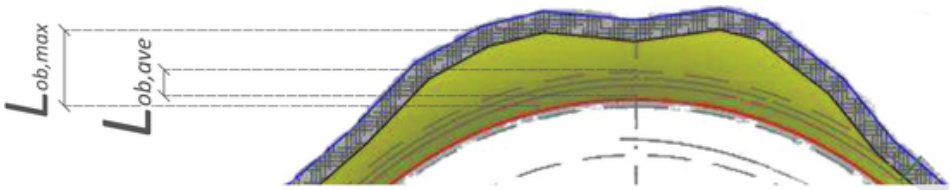

Fig. 11. Graphical identification of measured average ($L_{ob,ave}$) and maximum ($L_{ob,\max}$) thickness of overbreak.

Table 8
Experimental correlation between the average and maximum thickness of the overbreak with the length of blast holes and the *RMR* index.

Correlation coefficient ρ (data support 5 m)	Average thickness of the overbreak$L_{ob,ave}$	Maximum thickness of the overbreak $L_{ob,\max}$
Length of the blast holes L_{blast}	+0.68	–
Rock-mass rating *RMR*	–	−0.67

Table 9
Comparison of different models used for regression statistical analysis on the average and maximum thickness of overbreak.

Determination coefficient R^2 (data support 5 m)	Regression of $L_{ob,ave}$ *on* L_{blast}	Regression of $L_{ob,\max}$ on *RMR*
Linear model	0.4609	0.4479
Logarithmic model	0.4765	0.4266
Power model	0.4688	0.4328

Table 10
Initial values chosen for the non-linear regression analysis.

Parameters	Initial values
A	+0.0296
B	+0.4634
C	−0.1035
D	+0.4660

old, thus proving to be the less stable parameter of all (Table 11). Since the parameter *B* is linked to the L_{blast} in the proposed model of Equation (5), its instability showed that predictions of technical overbreak by using the length of the blast hole are consistently uncertain.

Another factor influencing the quality of the estimates is the number of data. A forward regression analysis was therefore performed to verify the stability of the results with reference to the number of measurements used for the calculation. This procedure allows the identification of the minimum number of data needed for a stable and accurate identification of the model parameters through the non-linear regression. Results are presented in Table 12 (all values), Fig. 12 (evolution of parameters' estimations with the number of measurements) and Fig. 13 (evolution of parameters' standard deviation with the number of measurements). Graphically, the threshold of 0.2 was considered an acceptable standard deviation value, which means the results become stable by using at least 60 measurements. However, an initial stabilisation of results can already be observed starting from 30 measurements.

4. Discussion

The new overbreak model (Equation (5)) was subsequently applied to the two other tunnels (CE and GLOS) as a validation exercise. Inspection of Fig. 14 shows that the new regression model well approximates the total overbreak as well as the geological and technical components, especially for the GLOS tunnel. A preliminary explanation of that resides in the fact that GA and GLOS are similar in size (see Table 4) and the data were in both cases collected almost exclusively while crossing the Brixner granite (see Fig. 4). For both tunnels, the new overbreak model returns a more precise fit for geological than for technical overbreak. This is coherent with the results of the forward regression, which evidenced, through the *B* parameter, that technical overbreak is the less stable part of the model.

Table 13 summarises the Root Mean Square Error (RMSE) found for the quantities *OB*, OB_{tec} and OB_{geo} for both CE and GLOS tunnels. RMSE is a common indicator of the total difference between the values predicted by the model and the ones observed.

It can be argued that the proposed analytical equation well approximates the evolution of total overbreak in the CE and GLOS tunnels, with a total value of the RMSE equal to 0.23 and 0.18, respectively. Furthermore, the specific geological overbreak is significantly better described than the technical one. This fact should be put in relation to the difficulties raised in the stabilisation of the *B* parameter of the model, representing the influence of the length of the blast holes.

The proposed model, even if apparently simple, seems quite robust and potentially applicable to further estimates of volume overbreak starting from drill-and-blast and geomechanical variables. Unlike previous attempts to predict blast-induced overbreak, it is able to clearly differentiate technical from geological components, an important aspect in the definition of contracts. The use of the TLS technique is functional to the application of the proposed model, since the scan of the tunnel sections allows the identification of the different overbreak thicknesses, thus verifying the model prediction accuracy along advancement of the excavation.

However, it should be stressed that the equation can be considered valid only under the following initial hypotheses:

Table 11
Results of the iterative procedure of the multiparameter non-linear regression NC = not calculated, fixed the parameter at the value of the previous step.

	First step		Second step		Third step	
Parameter	Estimation	Standard Deviation	Estimation	Standard Deviation	Estimation	Standard Deviation
A	0.039	0.006	NC	NC	NC	NC
B	0.243	0.154	0.233	0.047	0.271	0.050
C	−0.027	0.018	NC	NC	NC	NC
D	0.138	0.078	0.138	0.002	NC	NC

NC = not calculated, fixed the parameter at the value of the previous step.

Table 12
Estimations and related standard deviations in the forward regression analysis.

	Parameters							
	A		*B*		*C*		*D*	
Number of measurements	Estimation	Standard Deviation	Estimation	Standard Deviation	Estimation	Standard Deviation	Estimation	Standard Deviation
10	0.035	0.019	0.309	1.088	0.187	0.114	−0.808	0.501
20	0.042	0.013	0.559	0.607	0.182	0.054	−0.788	0.238
30	0.046	0.009	0.282	0.275	0.103	0.063	−0.438	0.277
40	0.045	0.009	0.212	0.251	−0.025	0.052	0.127	0.226
50	0.052	0.009	0.038	0.211	−0.018	0.046	0.096	0.201
60	0.050	0.007	0.003	0.158	−0.062	0.039	0.288	0.169
70	0.044	0.006	0.112	0.160	−0.033	0.032	0.159	0.138
80	0.045	0.006	0.048	0.161	−0.071	0.034	0.328	0.146
90	0.043	0.006	0.114	0.159	−0.074	0.032	0.343	0.138
100	0.039	0.006	0.233	0.047	−0.027	0.018	0.138	0.002

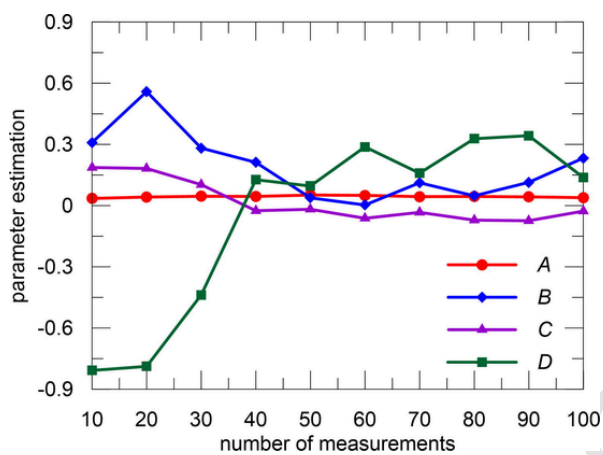

Fig. 12. Influence of the number of measurements on the parameters' estimation by forward regression.

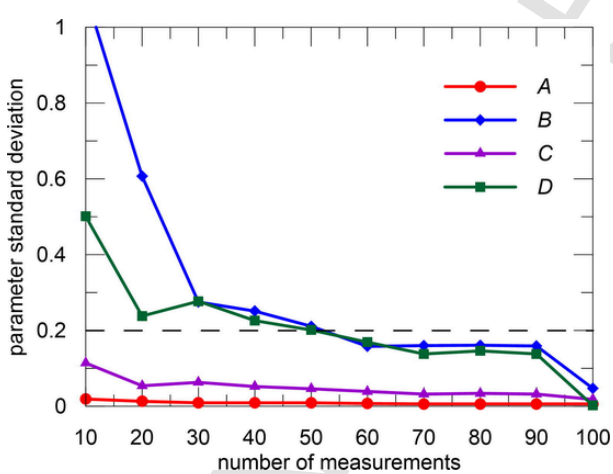

Fig. 13. Influence of the number of measurements on the parameters' standard deviation calculated by forward regression.

1. Excavation by drill-and-blast;
2. Characteristics of the blasting similar to those analysed in the study;
3. Use of smooth blasting to profile the tunnel contour.

A complete drill-and-blast excavation round generally lasts from 10 to 20 h, 25 to 50% of which are used for the removal of spoil material. In addition to the removal, the transportation and disposal of the excavated material also have a cost, which depends on many factors: type of rock, distance, necessity of crushing or milling and others. Table 14 shows the statistics of delay due to overbreak from the GA tunnel. Different section types were analysed. According to BBT classification, the "*T*" index represents the quality of rock-mass (*T1* = highest quality; *T5* = lowest quality); the "*Rb*" index indicates a possible risk of rock-burst; finally, the zones where transition of geomechanical conditions occur are identified by the indexes "*Mod*" (high transition) and "*TT*" (low transition). For each section, the time spent on the excavation rounds was measured and data were classified according to the presence or absence of significant overbreak. The minimum, average and maximum excavation time, with or without overbreak, were then calculated for each section type. An estimate of the average delay in construction related to the overbreak presence was then obtained. The data have showed an impact of overbreak on excavation time lying between 15% and 36%. The average delay due to the overbreak phenomenon is about 20%, with a standard deviation of 7% (Table 14).

Besides the loss of time due to the removal of spoil from the tunnel face, overbreak often implies the implementation of a series of additional safety measures, such as the installation of a wire mesh or radial swellex rock bolts, which has an additional impact on the excavation round timing.

High values of overbreak negatively affect the economy and the organisation of a tunnel construction. Overbreak mainly influences the variable costs of the excavation round, generally increasing them of about 10–15% (BBT, 2020).

5. Conclusions

The paper proposes an analysis of overbreak for tunnels excavated with the drill-and-blast method. In particular, the case study of the BBT system was considered and a total length of 1,806 m of excavation from three different tunnels was investigated.

Prediction of overbreak, with a reliable distinction between that due to geological factors and that related to technical aspects, is of high interest for the contractors and construction companies, giving the possibility to recognise in advance, with a certain degree of precision, the avoidable (mainly technical) and unavoidable (mainly geological) increased costs and additional times with respect to the preliminary previsions in the tunnel design phase.

Tunnel laser scanning was adopted to perform a detailed survey of the excavated surfaces and to estimate the volumes of overbreak. Moreover, the analysis of high-resolution images was useful to distinguish "geological" from "technical" overbreak, the latter clearly identified by the presence of half casts after the blasting. This approach aims at ef-

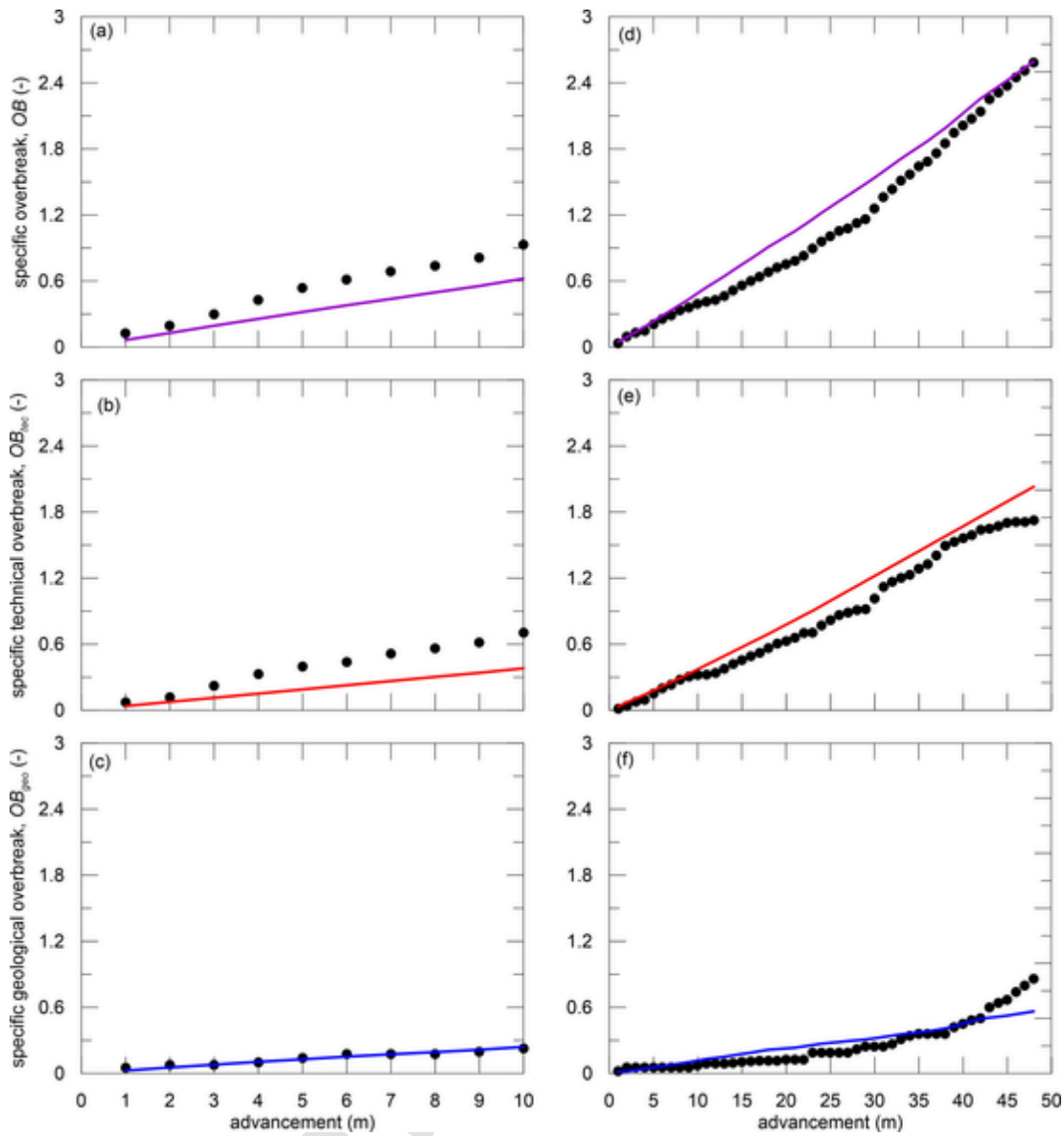

Fig. 14. Comparison between measured data and estimated trend for the different types of overbreak in the CE and GLOS tunnels.

Table 13
Root Mean Square Error between model results and measurements of specific overbreak in the two tunnel case studies (GLOS and CE).

RMSE (-)	CE	GLOS
Specific overbreak *OB*	0.23	0.18
Specific technical overbreak OB_{tec}	0.21	0.15
Specific geological overbreak OB_{geo}	0.02	0.09

fectively distinguishing the two types of overbreak, for the quantification of volumes and related amounts of costs to be eventually paid to the construction company.

The factors mainly influencing the overbreak are the *RMR* index for the geological overbreak and the length of the blast holes for the technical overbreak. The authors propose to use these two factors in a new empirical model for the prediction of the total volume of specific overbreak. The model was set up starting from the overbreak measurements on the first excavated tunnel and its prediction accuracy was then validated over the volumes in the two remaining tunnels. RMSE analysis between measured and predicted data proved the reliability of the model, especially for the estimation of the geological overbreak. However, at the present stage of research, the model can be considered valid only for tunnels constructed with a drill-and-blast technique similar to the one adopted in the BBT system.

Further validation and consequent generalisation of the proposed empirical model will require the investigation of different geomechanical contexts as well as the evaluation of geological and technical overbreak associated to other drilling geometries and blasting characteristics.

CRediT authorship contribution statement

G.M. Foderà: Methodology, Validation, Formal analysis, Investigation, Resources, Writing - original draft, Writing - review & editing, Visualization. **A. Voza:** Conceptualization, Supervision, Project administration. **G. Barovero:** Resources. **F. Tinti:** Methodology, Data curation, Writing - review & editing, Visualization. **D. Boldini:** Writing - review & editing, Supervision, Visualization, Project administration.

Table 14
Analysis of the excavation round for the GA tunnel and evidence of delay caused by overbreak.

Drill-and-blast excavation round for the GA tunnel									
Excavation specificities				Excavation round (h)					
Section type	Number of sections analysed	Effective average length (m)	RMR	Minimum time (h)	Maximum time (h)	Average time without overbreak (h)	Average time with overbreak (h)	Delay (h)	Percentage delay due to overbreak
GA-TRb	27	2.00	80	11.00	19.15	12.48	14.39	1.91	15.3%
GA-TRb$_{mod}$	11	2.00	78	10.35	18.03	13.27	18.03	4.76	35.9%
GA-T3 TT	52	3.00	76	13.24	26.11	15.46	18.07	2.61	16.9%
GA-T2	76	3.00	71	7.25	46.17	17.09	20.45	3.36	19.7%
GA-T3	110	3.00	71	10.36	28.16	18.09	22.00	3.91	21.6%
							Weighted average		20.1%
							Standard deviation		7.3%

Declaration of Competing Interest

The authors declare that they have no known competing financial interests or personal relationships that could have appeared to influence the work reported in this paper.

Acknowledgements

The research was made possible by a collaboration between BBT – Brenner Basis Tunnel SE and DICAM – Department of Civil, Chemical, Environmental and Materials Engineering of University of Bologna.

Appendix.

(see Fig. A1)

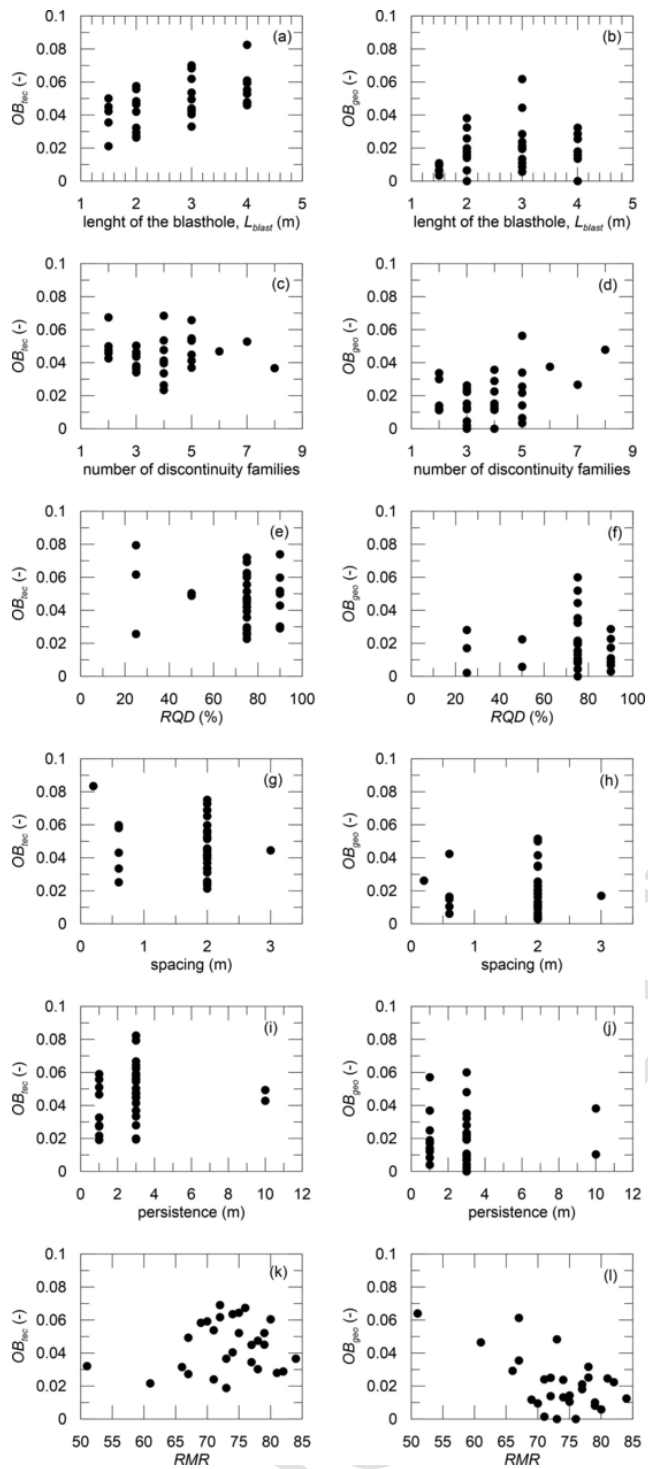

Fig. A1. Relation between technical factors and geological properties and measurements of technical and geological overbreak

References

Andersson P. 1992, Excavation disturbed zone in tunnelling. SveBeFo Report No. 8 Swedish Rock Engineering Research, Stockholm.

BBT 2020, Personal communication.

Boldini, D, Bruno, R, Egger, G, Staffisso, D, Voza, A, 2018. Statistical and Geostatistical Analysis of Drilling Parameters in the Brenner Base Tunnel. Rock Mech. Rock Eng. 51, 1955–1963.

Dey, K, Murthy, V M S R, 2012. Prediction of blast-induced overbreak from uncontrolled burn-cut blasting in tunnels driven through medium rock class. Tunn. Undergr. Sp. Tech. 28, 49–56.

Gong Feng-qiang (???), LI Xi-bing (???), ZHANG Wei (? ?) (2008), Over-excavation forecast of underground opening by using Bayes discriminant analysis method, J. Cent. South Univ. Technol., 15, 498–502.

Hoek, E, Brown, E T, 1980. Underground Excavations in Rock. Institution of Mining and Metallurgy, London, UK.

Ibarra, J A, Maerz, N H, Franklin, J A, 1996. Overbreak and underbreak in underground openings Part 2: Causes and Implications. Geotech. Geo.l Eng. 14, 325–340.

Innaurato, N, Mancini, R, Cardu, M, 1998. On the Influence of Rock Mass Quality on the Quality of Blasting Work in Tunnel Driving. Tunn. Undergr. Sp. Tech 89, 13.

Jang, H, Topal, E, 2013. Optimizing overbreak prediction based on geological parameters comparing multiple regression analysis and artificial neural network. Tunn. Undergr. Sp. Tech. 38, 161–169.

Kim, Y, Moon, H-K, 2013. Application of the guideline for overbreak control in granitic rock masses in Korean tunnels. Tunn. Undergr. Sp. Tech. 35, 67–77.

Levenberg, K, 1944. A Method for the Solution of Certain Non-Linear Problems in Least Squares. Quart. Appl. Math. 2 (2), 164–168.

Mahtab, M A, Rossler, K, Kalamaras, C S, Grasso, P, 1997. Assessment of geological overbreak for tunnel design and contractual claims. Int. J. Rock Mech. Min. 34, 3–4.

Mandal, S K, Singh, M M, 2009. Evaluating extent and causes of overbreak in tunnels. Tunn. Undergr. Sp. Tech 24, 22–36.

Marquardt, D, 1963. An Algorithm for Least-Squares Estimation of Nonlinear Parameters. SIAM J. Appl. Math. 11 (2), 431–441.

McKown, A, 1986. Perimeter control blasting for underground excavations in fractured and weathered rock. Environ. Eng. Geosci. 23 (4), 461–478.

Mohammadi, H, Barati, B, Yazdani, Chamzini A, 2018. Prediction of Blast-Induced Overbreak Based on Geo-mechanical Parameters, Blasting Factors and the Area of Tunnel Face. Geotech Geol Eng 36, 425–437.

Olsson M. and Berqgvist I. 1997 Crack propagation in rock from multiple hole blasting - summary of work during the period 1993-96. SveBeFo Report No. 32, Swedish Rock Engineering Research, Stockholm.

Saiang, D. 2008, Behaviour of Blast-Induced Damaged Zone Around Underground Excavations in Hard Rock Mass. Doctoral Thesis, Lulea University of Technology, Lulea, Sweden.

Schmitz R.M, Viroux S., Charlier R. and Hick S. 2006, The role of rock mechanics in analysing overbreak: application to the Soumagne tunnel, EUROCK 2006 – Multiphysics Coupling and Long Term Behaviour in Rock Mechanics

Singh, S P, Xavier, P, 2005. Causes, impact and control of overbreak in underground excavations. Tunn. Undergr. Sp. Tech 20, 63–71.

Sorce C., Cedrone L. and Lattanzi A. 2019, The Tunnel Laser Scanner technique: Applications to the road tunnel monitoring. In: Tunnels and Underground Cities: Engineering and Innovation meet Archaeology, Architecture and Art – Peila, Viggiani & Celestino (Eds), Taylor & Francis Group, London, ISBN 978-1-138-38864-9

Van Eldert, J, 2017. Measuring of Over-Break and the Excavation Damage Zone in Conventional Tunneling, World Tunnel Congress 2017. Bergen, Norway.

Verma, H K, Samadihya, N K, Singh, M, Goel, R K, Singh, P K, 2018. Blast induced rock mass damage around tunnels. Tunn. Undergr. Sp. Tech 71, 149–158.

Voza A., Valguarnera L., Fuoco S., Ascari G., Boldini D., Buttafoco D. 2020, A new methodology for the rock-burst assessment during tunnel construction, In Geotechnical Research for Land Protection and Development, Lecture Notes in Civil Engineering, Calvetti et al. eds, vol. 40, 668-677.

Widodo, S, Anwar, H, Syafitri, N A, 2019. Comparative analysis of ANFO and emulsion application on overbreak and underbreak at blasting development activity in underground Deep Mill Level Zone (DMLZ) PT Freeport IndonesiaI, OP Conf. Ser.: Earth. Environ. Sci. 279 (1), 012001.